



Editor: **Walid A. Daoud**

Self-Cleaning  
**MATERIALS  
AND SURFACES**

**A Nanotechnology Approach**

**WILEY**

# Self-Cleaning Materials and Surfaces

## A Nanotechnology Approach

Edited by

WALID A. DAOUD

*School of Energy and Environment, City University of Hong Kong,  
Hong Kong*

1.2.2	Other Factors	17
1.2.3	Nature's Answers	17
1.2.4	Superhydrophilic Self-Cleaning Surfaces	19
1.2.5	Functional Properties of Superhydrophilic Surfaces	30
1.3	Materials and Fabrication	25
1.4	Future Perspectives	27
	References	31

## PART II APPLICATIONS OF SELF-CLEANING SURFACES

2	Recent Development on Self-Cleaning Cementitious Composites	33
2.1	Introduction	33
2.2	Atmospheric Pollution: Substances and Laws	35
2.2.1	Nitrogen Oxides	36
2.2.2	Particulate Matter	37
2.2.3	Volatile Organic Compounds	37
2.3	Heterogeneous Photocatalysis	38

**WILEY**

This edition first published 2013  
© 2013 John Wiley & Sons, Ltd

*Registered office*

John Wiley & Sons Ltd, The Atrium, Southern Gate, Chichester, West Sussex, PO19 8SQ, United Kingdom

For details of our global editorial offices, for customer services and for information about how to apply for permission to reuse the copyright material in this book please see our website at [www.wiley.com](http://www.wiley.com).

The right of the author to be identified as the author of this work has been asserted in accordance with the Copyright, Designs and Patents Act 1988.

All rights reserved. No part of this publication may be reproduced, stored in a retrieval system, or transmitted, in any form or by any means, electronic, mechanical, photocopying, recording or otherwise, except as permitted by the UK Copyright, Designs and Patents Act 1988, without the prior permission of the publisher.

Wiley also publishes its books in a variety of electronic formats. Some content that appears in print may not be available in electronic books.

Designations used by companies to distinguish their products are often claimed as trademarks. All brand names and product names used in this book are trade names, service marks, trademarks or registered trademarks of their respective owners. The publisher is not associated with any product or vendor mentioned in this book. This publication is designed to provide accurate and authoritative information in regard to the subject matter covered. It is sold on the understanding that the publisher is not engaged in rendering professional services. If professional advice or other expert assistance is required, the services of a competent professional should be sought.

The publisher and the author make no representations or warranties with respect to the accuracy or completeness of the contents of this work and specifically disclaim all warranties, including without limitation any implied warranties of fitness for a particular purpose. This work is sold with the understanding that the publisher is not engaged in rendering professional services. The advice and strategies contained herein may not be suitable for every situation. In view of ongoing research, equipment modifications, changes in governmental regulations, and the constant flow of information relating to the use of experimental reagents, equipment, and devices, the reader is urged to review and evaluate the information provided in the package insert or instructions for each chemical, piece of equipment, reagent, or device for, among other things, any changes in the instructions or indication of usage and for added warnings and precautions. The fact that an organization or Website is referred to in this work as a citation and/or a potential source of further information does not mean that the author or the publisher endorses the information the organization or Website may provide or recommendations it may make. Further, readers should be aware that Internet Websites listed in this work may have changed or disappeared between when this work was written and when it is read. No warranty may be created or extended by any promotional statements for this work. Neither the publisher nor the author shall be liable for any damages arising herefrom.

***Library of Congress Cataloging-in-Publication Data***

Self-cleaning materials and surfaces : a nanotechnology approach / edited by Walid A. Daoud.

pages cm

Includes bibliographical references and index.

ISBN 978-1-119-99177-9 (cloth)

1. Coatings. 2. Surface active agents. 3. Materials-Cleaning. 4. Nanostructured materials. I. Daoud, Walid A.

TA418.9.C57S45 2013

667'.9-dc23

2013016955

A catalogue record for this book is available from the British Library.

ISBN: 9781119991779

Set in 10/12pt Times by Aptara Inc., New Delhi, India.

Printed and bound in Malaysia by Vivar Printing Sdn Bhd

# Contents

*List of Contributors*

xiii

*Preface*

xv

## PART I CONCEPTS OF SELF-CLEANING SURFACES

<b>1</b>	<b>Superhydrophobicity and Self-Cleaning</b>	<b>3</b>
	<i>Paul Roach and Neil Shirtcliffe</i>	
1.1	Superhydrophobicity	3
1.1.1	Introducing Superhydrophobicity	3
1.1.2	Contact Angles and Wetting	4
1.1.3	Contact Angle Hysteresis	4
1.1.4	The Effect of Roughness on Contact Angles	6
1.1.5	Where the Equations Come From	8
1.1.6	Which State Does a Drop Move Into?	11
1.2	Self-Cleaning on Superhydrophobic Surfaces	12
1.2.1	Mechanisms of Self-Cleaning on Superhydrophobic Surfaces	12
1.2.2	Other Factors	15
1.2.3	Nature's Answers	17
1.2.4	Superhydrophilic Self-Cleaning Surfaces	19
1.2.5	Functional Properties of Superhydrophobic Surfaces	20
1.3	Materials and Fabrication	25
1.4	Future Perspectives	27
	References	28

## PART II APPLICATIONS OF SELF-CLEANING SURFACES

<b>2</b>	<b>Recent Development on Self-Cleaning Cementitious Coatings</b>	<b>35</b>
	<i>Daniele Enea</i>	
2.1	Introduction	35
2.2	Atmospheric Pollution: Substances and Laws	36
2.2.1	Nitrogen Oxides	36
2.2.2	Particulate Matter	37
2.2.3	Volatile Organic Compounds	37
2.3	Heterogeneous Photocatalysis	38

2.4	Self-Cleaning Surfaces	39
2.4.1	Mechanisms of Photo-Reduction of Air Pollutants	41
2.4.2	Some Experimental Evidences	41
2.5	Main Applications	44
2.6	Test Methods	46
2.6.1	Colour	46
2.6.2	Photocatalytic Degradation of Nitrogen Oxides	47
2.6.3	Photocatalytic Degradation of Micro-Pollutants in Air	49
2.6.4	Photocatalytic Degradation of Rhodamine B	51
2.6.5	Spectroscopic Techniques	53
2.7	Future Developments	53
	References	54
<b>3</b>	<b>Recent Progress on Self-Cleaning Glasses and Integration with Other Functions</b>	<b>57</b>
	<i>Baoshun Liu, Qingnan Zhao and Xiujian Zhao</i>	
3.1	Introduction	57
3.2	Theoretical Fundamentals for Self-Cleaning Glasses	58
3.2.1	Wettability	58
3.2.2	Photoinduced Hydrophilicity	59
3.2.3	Heterogeneous Photocatalysis	62
3.3	Self-Cleaning Glasses Based on Photocatalysis and Photoinduced Hydrophilicity	63
3.3.1	Self-Cleaning Glasses with Pores	63
3.3.2	Doping to Realize Visible-Light-Induced Self-Cleaning Glasses	65
3.3.3	The Use of Hole Transfer to Realize Self-Cleaning	67
3.3.4	The Effect of Temperature and Atmosphere on the Photoinduced Hydrophilicity	67
3.3.5	The Effect of Soda Ions on the Properties of Self-Cleaning Glasses	69
3.3.6	The Anti-Bacterial Effect and Anti-Fogging Effect	70
3.3.7	The Composite SiO <sub>2</sub> Films for Self-Cleaning Glasses with High Antireflection	72
3.4	Inorganic Hydrophobic Self-Cleaning Glasses	75
3.4.1	Modifying The TiO <sub>2</sub> Film by Low-Electronegativity Elements	75
3.4.2	The Application of ZnO Material in a Superhydrophobic Material	77
3.5	Self-Cleaning Glasses Modified by Organic Molecules	79
3.6	The Functionality of Self-Cleaning Glasses	80
	References	84
<b>4</b>	<b>Self-Cleaning Surface of Clay Roofing Tiles</b>	<b>89</b>
	<i>Jonjaua Ranogajec and Miroslava Radeka</i>	
4.1	Clay Roofing Tiles and Their Deterioration Phenomena	89
4.1.1	Raw Material Composition and Firing Process	89



4.1.2	Surface Characteristics of Clay Roofing Tiles	91
4.1.3	Frost, Chemical and Biocorrosion Deterioration of Clay Roofing Tiles	96
4.1.4	Simulation of Weathering of Clay Roofing Tiles in Laboratory Conditions	97
4.2	Protective and Self-Cleaning Materials for Clay Roofing Tiles	105
4.2.1	Design of Protective and Self-Cleaning Coatings	107
4.2.2	Monitoring the Characteristics of Coated Clay Roofing Tiles	113
	References	123
<b>5</b>	<b>Self-Cleaning Fibers and Fabrics</b>	<b>129</b>
	<i>Wing Sze Tung and Walid A. Daoud</i>	
5.1	Introduction	129
5.2	Photocatalysis	130
5.2.1	Mechanisms	131
5.2.2	Titanium Dioxide Photocatalyst	132
5.3	Photocatalytic Self-Cleaning Surface Functionalization of Fibrous Materials	134
5.3.1	Self-Cleaning Cellulosic Fibers	134
5.3.2	Self-Cleaning Keratin Fibers	139
5.3.3	Self-Cleaning Synthetic Fibers	140
5.4	Application of Photocatalytic Self-Cleaning Fibers	142
5.4.1	Protective Clothing	142
5.4.2	Household Appliances and Interior Furnishing	143
5.5	Limitations	144
5.5.1	Environmental Concerns	144
5.5.2	Human Safety Concerns	144
5.5.3	Photocatalytic Efficiency and Stability	145
5.6	Future Prospects	146
5.6.1	Visible Light Activation	146
5.6.2	Remote Photocatalytic Effect	146
5.6.3	Process Modification	146
5.6.4	Empirical Measurements	147
5.7	Conclusions	147
	References	147
<b>6</b>	<b>Self-Cleaning Materials for Plastic and Plastic-Containing Substrates</b>	<b>153</b>
	<i>Houman Yaghoubi</i>	
6.1	Introduction	153
6.2	TiO <sub>2</sub> Thin Films on Polymers: Sol-Gel-Based Wet Coating Techniques	155
6.2.1	Wet Coating Techniques: History and Advantages	155
6.2.2	TiO <sub>2</sub> Photocatalytic Thin Films on PC and PMMA	156
6.2.3	SiO <sub>2</sub> Incorporation into TiO <sub>2</sub> - SiO <sub>2</sub> as an Interfacial Layer for TiO <sub>2</sub>	162
6.2.4	TiO <sub>2</sub> Photocatalytic Thin Films on PET and HDPE	167

6.2.5	TiO <sub>2</sub> Photocatalytic Thin Films on PS	171
6.2.6	Modified Hybrid TiO <sub>2</sub> Sols on Plastics: ABS, Polystyrene, and PVC	172
6.2.7	TiO <sub>2</sub> on Paints and Self-Cleaning Paints	175
6.2.8	MW Irradiation-Assisted Dip Coating for Low-Temperature TiO <sub>2</sub> Deposition on Polymers	178
6.2.9	Nanomechanical Properties of Dipped TiO <sub>2</sub> Granular Thin Films on Polymer Substrates	179
6.3	TiO <sub>2</sub> -Polymer Nanocomposites Review: Casting (Mixing) Techniques	181
6.3.1	Short History and Advantages	181
6.3.2	Ag/Polyethylene Glycol (PEG)-Polyurethane (PU)-TiO <sub>2</sub> Nanocomposite Films by Solution Casting Techniques	182
6.3.3	Antimicrobial Activity of TiO <sub>2</sub> -Isotactic Polypropylene (iPP) Composites	183
6.3.4	TiO <sub>2</sub> Immobilized Biodegradable Polymers	184
6.4	TiO <sub>2</sub> Sputter-Coated Films on Polymer Substrates	187
6.4.1	DC Reactive Magnetron Sputtering of Photocatalytic TiO <sub>2</sub> Films on PC	187
6.4.2	Reactive Radio-Frequency [RF] Magnetron Sputtering of Photocatalytic TiO <sub>2</sub> Films on PET	189
6.5	TiO <sub>2</sub> Thin Films on PET and PMMA by Nanoparticle Deposition Systems (NPDS)	190
6.6	Photo-Responsive Discharging Effect of Static Electricity on TiO <sub>2</sub> -Coated Plastic Films	192
6.7	Recent Achievements	192
6.7.1	Commercialized Products: Ube-Nitto Kasei Co. and the University of Tokyo	192
6.7.2	Patents: University of Wisconsin	193
	Acknowledgements	194
	References	194

### PART III ADVANCES IN SELF-CLEANING SURFACES

7	<b>Self-Cleaning Textiles Modified by TiO<sub>2</sub> and Bactericide Textiles Modified by Ag and Cu</b>	<b>205</b>
	<i>John Kiwi and Cesar Pulgarin</i>	
7.1	Introduction	205
7.2	Self-Cleaning Textiles: RF-Plasma Pretreatment to Increase the Binding of TiO <sub>2</sub>	206
7.3	Self-Cleaning Mechanism for Colorless and Colored Stains on Textiles	208
7.4	Self-Cleaning Textiles: Vacuum-UVC Pretreatment to Increase the Binding of TiO <sub>2</sub>	209

7.5	XPS to Follow Stain Discoloration on Cotton Modified with TiO <sub>2</sub> and Characterization of the TiO <sub>2</sub> Coating	212
7.6	Bactericide/Ag/Textiles Prepared by Pretreatment with Vacuum-UVC	214
7.7	DC-Magnetron Sputtering of Textiles with Ag Inactivating Airborne Bacteria	217
7.8	Inactivation of <i>E. coli</i> by CuO in Suspension in the Dark and Under Visible Light	218
7.9	Inactivation of <i>E. coli</i> by Pretreated Cotton Textiles Modified with Cu/CuO at the Solid/Air Interface	220
7.10	Direct Current Magnetron Sputtering (DC and DCP) of Nanoparticulate Continuous Cu-Coatings on Cotton Textile Inducing Bacterial Inactivation in the Dark and Under Light Irradiation	220
7.11	Future Trends	223
	References	224
<b>8</b>	<b>Liquid Flame Spray as a Means to Achieve Nanoscale Coatings with Easy-to-Clean Properties</b>	<b>229</b>
	<i>Mikko Aromaa, Joe A. Pimenoff and Jyrki M. Mäkelä</i>	
8.1	Gas-Phase Synthesis of Nanoparticles	229
8.2	Aerosol Reactors	233
8.2.1	Hot Wall Reactors	233
8.2.2	Laser Reactors	234
8.2.3	Plasma Reactors	234
8.2.4	Flame Reactors	235
8.2.5	Spray Pyrolysis	236
8.3	Liquid Flame Spray	237
8.3.1	Synthesis of Nanoparticles via LFS	237
8.3.2	Multicomponent Nanoparticles	238
8.3.3	Synthesis and Deposition of Nanoparticle Coatings	240
8.4	Liquid Flame Spray in Synthesis of Easy-to-Clean Antimicrobial Coatings	243
8.4.1	Synthesis of Titanium Dioxide	243
8.4.2	Deposition of the Titania Coatings	244
8.4.3	Doping of the Coatings	246
8.4.4	Performance of the Antimicrobial Easy-to-Clean Coatings	247
8.5	Summary	249
	References	249
<b>9</b>	<b>Pulsed Laser Deposition of Surfaces with Tunable Wettability</b>	<b>253</b>
	<i>Evie L. Papadopolou</i>	
9.1	Introduction	253
9.2	Basic Theory of Wetting Properties of Surfaces	254
9.2.1	Planar Surfaces	254
9.2.2	Rough Surfaces	255



9.3	Roughening a Flat Surface	256
9.3.1	PLD Technique Overview	257
9.3.2	Nanostructures Grown by PLD	257
9.4	Switchable Wettability	263
9.4.1	Photoinduced Wettability on PLD Structures	263
9.4.2	Electrowetting on PLD Structures	267
9.5	Concluding Remarks	270
	References	271
<b>10</b>	<b>Fabrication of Antireflective Self-Cleaning Surfaces Using Layer-by-Layer Assembly Techniques</b>	<b>277</b>
	<i>Yu-Min Yang</i>	
10.1	Introduction	277
10.2	Antireflective Coatings	278
10.2.1	Interference Multiple Layers	278
10.2.2	Inhomogeneous Layer with Gradient Refractive Index	279
10.3	Solution-Based Layer-by-Layer (LbL) Assembly Techniques	280
10.3.1	Electrostatic Assembly	280
10.3.2	Langmuir-Blodgett (LB) Assembly	281
10.3.3	Self-Assembly	282
10.4	Mechanisms of Self-Cleaning	283
10.4.1	Hydrophilic Surfaces	283
10.4.2	Hydrophobic Surfaces	284
10.5	Fabrication of Antireflective Self-Cleaning Surfaces Using Electrostatic Layer-by-Layer (ELbL) Assembly of Nanoparticles	285
10.5.1	Superhydrophilic Self-Cleaning Surfaces with Antireflective Properties	285
10.5.2	Superhydrophobic Self-Cleaning Surfaces with Antireflective Properties	291
10.6	Fabrication of Superhydrophobic Self-Cleaning Surfaces Using LB Assembly of Micro-/Nanoparticles	297
10.7	Characterization of As-Fabricated Surfaces	300
10.7.1	Surface Morphology and Roughness	300
10.7.2	Thickness, Porosity, and Refractive Index	301
10.7.3	Transmittance	302
10.7.4	Photocatalytic Properties	303
10.7.5	Contact Angle and Contact Angle Hysteresis	304
10.7.6	Mechanical Stability	305
10.8	Challenges and Future Development	306
10.9	Conclusion	307
	References	307

## PART IV POTENTIAL HAZARDS AND LIMITATIONS OF SELF-CLEANING SURFACES

<b>11 The Environmental Impact of a Nanoparticle-Based Reduced Need of Cleaning Product and the Limitation Thereof</b>	<b>315</b>
<i>L. Reijnders</i>	
11.1 Introduction	315
11.1.1 Outline	315
11.1.2 Nanoparticle-Based Reduced Need of Cleaning Surfaces	316
11.2 Titania and Amorphous Silica Nanoparticles and Carbon Nanotubes Can Be Hazardous and May Pose a Risk	319
11.2.1 Molecular Mechanisms	322
11.2.2 Risk Caused by Nanoparticles	322
11.3 Environmental Impact of a Reduced Need of Cleaning Product	323
11.3.1 Direct Environmental Effects of a Nanoparticle-Based Reduced Need of Cleaning Product	324
11.3.2 Net Direct Environmental Benefits	328
11.3.3 Indirect Environmental Effects of a Nanoparticle-Based Reduced Need of Cleaning Product	329
11.4 Limiting the Direct Environmental Impact of a Nanoparticle-Based Reduced Need of Cleaning Product, Including Limitation of Risks Following from Exposure to Nanoparticles	330
11.4.1 Limiting the Direct Environmental Impact	330
11.4.2 Limitation of Risks Following from Exposure to Nanoparticles	330
11.5 Conclusion	331
References	331
<b>Index</b>	<b>347</b>

*Enzo L. Papadopoulos, Institute of Electronic Structures and Lasers, Foundation for Research and Technology (IIT), Greece. Current address: Istituto Italiano di Tecnologia, Genova, Italy*

*Jouko A. Pienimäki, Helsing Oy, Vantaa, Finland*

*César Pulgarin, Institute of Chemical Sciences and Engineering, Swiss Federal Institute of Technology Lausanne (EPFL), Switzerland*

*Miroslava Radetka, Faculty of Technical Sciences, University of Novi Sad, Serbia*

*Josipina Rantogajec, Faculty of Technology, University of Novi Sad, Serbia*

*L. Reijnders, Institute for Biodiversity and Ecosystem Dynamics, University of Amsterdam, The Netherlands*

*Paul Roach, Institute for Science and Technology in Medicine, Guy Hillon Research Centre, Keele University, UK*

## List of Contributors

**Mikko Aromaa**, Aerosol Physics Laboratory, Department of Physics, Tampere University of Technology, Finland

**Walid A. Daoud**, School of Energy and Environment, City University of Hong Kong, Hong Kong

**Daniele Enea**, Department of Architecture, University of Palermo, Italy

**John Kiwi**, Institute of Chemical Sciences and Engineering, Swiss Federal Institute of Technology Lausanne (EPFL), Switzerland

**Baoshun Liu**, State Key Laboratory of Silicate Materials for Architectures, Wuhan University of Technology, PR China and School of Material Science and Engineering, Wuhan University of Technology, PR China

**Jyrki M. Mäkelä**, Aerosol Physics Laboratory, Department of Physics, Tampere University of Technology, Finland

**Evie L. Papadopoulos**, Institute of Electronic Structures and Lasers, Foundation for Research and Technology-Hellas, Greece. Current address: Istituto Italiano di Tecnologia, Genova, Italy

**Joe A. Pimenoff**, Beneq Oy, Vantaa, Finland

**Cesar Pulgarin**, Institute of Chemical Sciences and Engineering, Swiss Federal Institute of Technology Lausanne (EPFL), Switzerland

**Miroslava Radeka**, Faculty of Technical Sciences, University of Novi Sad, Serbia

**Jonjaua Ranogajec**, Faculty of Technology, University of Novi Sad, Serbia

**L. Reijnders**, Institute for Biodiversity and Ecosystem Dynamics, University of Amsterdam, The Netherlands

**Paul Roach**, Institute for Science and Technology in Medicine, Guy Hilton Research Centre, Keele University, UK

**Neil Shirtcliffe**, Faculty of Technology and Bionics, Hochschule Rhein-Waal, Germany

**Wing Sze Tung**, School of Applied Sciences and Engineering, Monash University, Australia

**Houman Yaghoubi**, Department of Mechanical Engineering/Department of Electrical Engineering, University of South Florida, USA

**Yu-Min Yang**, Department of Chemical Engineering, National Cheng Kung University, Taiwan

**Qingnan Zhao**, State Key Laboratory of Silicate Materials for Architectures, Wuhan University of Technology, PR China

**Xiujian Zhao**, State Key Laboratory of Silicate Materials for Architectures, Wuhan University of Technology, PR China

# Recent Development on Self-Cleaning Cementitious Coatings

Daniele Enea

*Department of Architecture, University of Palermo, Italy*

## 2.1 Introduction

The increased interest in the sustainability of the whole building process, ruled and controlled by a regulatory and legal system, is increasingly changing management strategies in construction, favouring a preventive policy instead of widespread intervention when breakdown occurs. This new approach requires knowledge of the durability of materials and building components and their ability to maintain acceptable performance characteristics over time.

Reducing maintenance costs, focusing attention on the external building envelope, requires surfaces to be more durable. To address this issue, the scientific community, together with the construction industry, has, in the last two decades, carried out studies and research to improve the performance of building surfaces.

Nanotechnologies have introduced significant innovations in several fields, particularly in the building construction one, where the application of a new technology based on photocatalysis has aroused increasing interest in the scientific community.

The discovery of the different behaviour of matter at the macroscale and nanoscale is at the base of nanotechnology; different laws rule at different scales, leading to changes in properties with size.

Nanotechnology deals with the electronic properties and the electronic effects of nano-materials. Matter reduced in at least one dimension to a size less than 100 nm can be



considered as a nanomaterial. The reduction in size means nanomaterials have an increased surface area, a main aspect influencing and determining specific properties.

Nanotechnology is thus applied to modify the properties of matter, forming new materials with new properties, useful for environmental applications: from purification of industrial and vehicular exhaust emissions, to the clean and renewable solar energy.

Photocatalysis is important in this regard and is applied to reduce environmental pollution.

This is a clean technology based on the use of solar energy, activating the photocatalytic principles dispersed on surfaces and able to contribute to the reduction of environmental pollution and energy consumption.

These innovative materials allow the acceleration of the reactions of chemical decomposition of atmospheric organic and inorganic pollutants and their availability in the construction building market is increasing. These materials – solid semiconductors – work by accelerating the oxidative process that leads to the complete mineralization of air pollutants which thus become harmless substances. The most commonly used solid semiconductor is titanium dioxide ( $\text{TiO}_2$ ), due to its widespread availability, its most efficient photoactivity, highest stability and lowest cost.

Seminal works in this area started in 1972, when the Fujishima–Honda effect was developed, consisting in the production of oxygen gas bubbles at an electrode of  $\text{TiO}_2$  placed in electrical contact with a piece of platinum metal, both immersed in water and exposed to light; at the platinum electrode was observed the production of hydrogen [1]. The study showed that  $\text{TiO}_2$  subjected to a light source has a strong oxidant power, because it can oxidize water to oxygen gas.

Other research, carried out especially in Japan, showed interesting results regarding the capability of  $\text{TiO}_2$  to oxidize almost all types of organic compounds.

The electronic and optical properties of  $\text{TiO}_2$  have several applications in gas sensors, antireflection coatings for solar cells, antibacterial filters, nano-films and, most noteworthy, in the superhydrophilic and self-cleaning glass and building surfaces.

Due to their extent and the limited costs to be covered by innovative photocatalytic materials, these surfaces are the most suitable.

## **2.2 Atmospheric Pollution: Substances and Laws**

Among atmospheric pollutants, the most dangerous for human health are nitrogen dioxide ( $\text{NO}_2$ ), volatile organic compounds (VOCs) and particulate matter (PM).

### **2.2.1 Nitrogen Oxides**

Nitrogen dioxide is a toxic gas, absorbing visible solar radiation and contributing to impaired atmospheric visibility. It absorbs visible radiation and has a potentially direct role in global climate change and plays a critical role in determining ozone concentrations in the troposphere.

It is produced by the oxidation of nitric oxide in the atmosphere; this reaction commonly occurs in most combustion processes. Moreover, large-scale production of nitrogen oxides ( $\text{NO}_x$ ) is due to internal combustion engines, particularly concentrated in congested urban areas, and stationary sources (heating and power generation).

The World Health Organization (WHO) has investigated  $\text{NO}_2$ , finding adverse health effects even when the annual average nitrogen dioxide concentration complied with the WHO annual guideline [2] value of  $40 \mu\text{g m}^{-3}$ .

### 2.2.2 Particulate Matter

Airborne particulate matter is a complex mixture of components with different chemical and physical characteristics. Due to this heterogeneity, it is impossible to unambiguously establish health risks, without a correlation with particle size, source and chemical composition.

Particulate matter is classified by aerodynamic diameter, as size is a critical determinant of the likelihood and site of deposition within the respiratory tract, so it is often designated as  $\text{PM}_{10}$  and  $\text{PM}_{2.5}$ , with particle diameters 10 and  $2.5 \mu\text{m}$ , respectively. The two indicators differ for thoracic coarse mass particulate matter and  $\text{PM}_{10}$  includes these bigger particles and  $\text{PM}_{2.5}$ .

$\text{PM}_{2.5}$  is more dangerous than  $\text{PM}_{10}$ , as there is a high probability of deposition in the smaller conducting airways and alveoli.

In urban environments, it is possible to find even ultrafine particles, smaller than  $0.1 \mu\text{m}$  (100 nm), different in particle mass, origin, physical characteristics and chemical composition.

The largest particles of  $\text{PM}_{10}$  are mechanically produced by the break-up of solid particles and often adhere to biological matter, thus containing dust from roads and industrial activities, and biological matter such as pollen grains and bacterial fragments. Coarse particles may also be formed from the incomplete combustion of vehicular engines and electric plants and are known as fly ash.

$\text{PM}_{2.5}$  is derived from gases, but combustion processes may also generate primary particles in this size range. Typically, these particles originate as ultrafine particles produced by nucleation-condensation of low-vapour-pressure substances formed by high-temperature vaporization or by chemical reactions in the atmosphere.

The smaller particles ( $<0.1 \mu\text{m}$ ) can also be produced by the condensation of metals or organic compounds that are vaporized in high-temperature combustion processes, and by the condensation of gases (sulfur dioxide, nitrogen oxides, ammonia and volatile organic compounds) that atmospheric reactions convert into low-vapour-pressure substances.

The injurious effects on human health are proved and increase with exposure, affecting the respiratory and cardiovascular systems.

A threshold of  $10 \mu\text{g m}^{-3}$  for  $\text{PM}_{2.5}$  was chosen to represent the lower end of the range over which significant effects on survival have been observed in an American Cancer Society (ACS) study [3].

### 2.2.3 Volatile Organic Compounds

Volatile organic compounds represent a very wide range of hydrocarbons, oxygenates, halogenates and other carbon compounds existing in the atmosphere in the vapour phase. The main source is through leakage from pressurized systems (e.g. natural gas, methane) or evaporation of a liquid fuel, such as benzene, from the fuel tank of a vehicle. However, combustion of fossil fuels and incineration processes also create combustion emissions containing unburned fuel fragments, emitted in the form of VOC [4].

The most dangerous one is benzene, a colourless and highly flammable liquid with a sweet smell, which has potential health effects from long-term exposure causing anaemia, decrease in blood platelets and increased risk of cancer.

The US Occupational Safety and Health Administration (OSHA) set an acceptable exposure limit of 1 part of benzene per million parts of air (1 ppm) in the workplace during an 8-hour workday, 40-hour work-week. The short term exposure limit for airborne benzene is 5 ppm for 15 min [5].

European Directives 1999/30/CE and 2000/69/CE imposed on all members limits for nitrogen oxides, particulate matter and benzene in the atmospheric air: limits that should have been reduced gradually. Particularly, annual limits were fixed to  $40 \mu\text{g m}^{-3}$  for  $\text{NO}_2$  and should have been reduced to zero by 1 January 2010, the same limit was fixed for  $\text{PM}_{10}$  and its reduction to zero had to be by 1 January 2005, and  $5 \mu\text{g m}^{-3}$  for benzene reduced to zero by 1 January 2010.

### 2.3 Heterogeneous Photocatalysis

Photocatalysis is a photochemical process of catalysis under light irradiation, leading to the acceleration of chemical reactions in the presence of a photocatalyst.

The photocatalyst, dispersed in the matrix, does not participate in the reaction, thus is not consumed by the reaction itself, but increases the rate of reaction through the action of light.

This process is characterized by the different phases of the catalyst, typically in the solid phase, and the reactants in the gas or liquid phase [6], this is the reason why photocatalysis is called heterogeneous.

The reactants come into contact with the catalyst and are adsorbed onto its surface, then the chemical reactions take place and finally the products are desorbed from the surface and diffuse away.

These reactions are accelerated due to the semiconductor nature of the photocatalyst.

Because of their electronic structure, which is characterized by a full valence band (VB) and an empty conduction band (CB), semiconductors ( $\text{TiO}_2$ ,  $\text{ZnO}$ ,  $\text{CdS}$ , etc.) can activate photo-induced redox processes.

The difference between the lowest energy level of the CB and the higher energy level of the VB is the so-called "energy gap",  $E_g$ . It corresponds to the minimum energy required to make a material a conductor.

Ultraviolet light gives the minimum energy required to make these photoreactions possible, as shown in Figure 2.1.

Three main mechanisms can promote this electron flow: thermal excitation, doping and photo-excitation.

Among others, photo-excitation occurs when the promotion of the electron ( $e^-$ ) to the conduction band is due to absorption of a photon of light, with  $h\nu > E_g$ . In this case, a hole ( $h^+$ ) remains in the valence band, so these electron-hole pairs diffuse on the surface of the photocatalytic particle, participating in chemical reactions with the adsorbed molecules.

Among others, titanium dioxide is the most used in photochemical processes due to its chemical stability, harmless nature and, compared to other semiconductor metal oxides, relative cheapness.

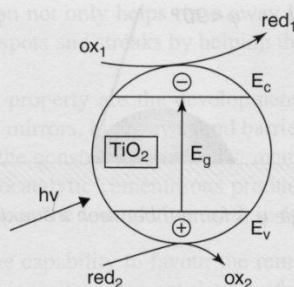
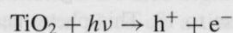


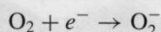
**Figure 2.1** The mechanism of photoreaction of a semiconductor particle.

The band gap of semiconductors is smaller than that of insulating materials, so radiation with energy greater than 3.2 eV for TiO<sub>2</sub> in the anatase form and 3.0 eV in the rutile form is able to promote electrons to the conduction band. This energy is often supplied by a non-electric source, such as heat or light.

Particularly, a quantum of light with wavelength lower than 380 nm, in the ultraviolet range, produces the electron–hole pairs, according to the equation:



The electron–hole pairs are able to react and decompose oxygen and water, present in the atmosphere, generating OH<sup>•</sup>, hydroxyl radicals, and O<sub>2</sub><sup>-</sup>, superoxide ions, according to the following equations:



These two powerful oxidizing agents will then disintegrate and rearrange the structure of some atmospheric pollutants and convert them, through redox reactions occurring on the surface of the catalyst, into limestone, nitrates and CO<sub>2</sub>, which are easily washed away by rain [7, 8].

## 2.4 Self-Cleaning Surfaces

Nowadays, there is no American (ASTM) or International (ISO) standard reporting a description of self-cleaning surfaces, but the term is commonly referred to the superhydrophilic and hydrophobic properties. These two characteristics of a surface are strictly related to the contact angle between liquid drops coming into contact with the surface itself, as shown in Figure 2.2.

The contact angle,  $\varphi$ , gives a quantitative measure of the wettability of a solid surface by a liquid and depends on the superficial tensions at the interface.

Low values of the contact angle mean the liquid spreads on the surface until the complete wetting of the surface when  $\varphi = 0$  and the surface is thus defined as hydrophilic.

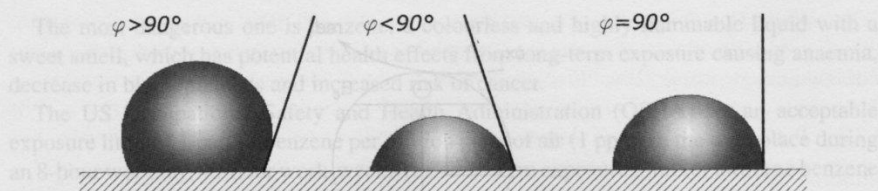


**Figure 2.2** The contact angle  $\phi$  is formed between a liquid drop and a solid surface.

The higher the contact angle, the poorer the wetting of the surface and the surface is then known as hydrophobic.

There is a range of values of contact angle between a solid surface and a liquid drop and it depends on the recent history of the interaction.

The Loto-effect is characteristic of the lotus leaves (Figure 2.3), a genus of aquatic plants of the Nelumbonaceae family, having a superhydrophobic property such that water drops in contact have a contact angle greater than  $130^\circ$ . This effect ensures the self-cleaning property. Pollutant particulate, in fact, adheres to these water drops, and is thus removed.

When titanium dioxide in the mineral form of anatase is irradiated by UV light, a superhydrophilic property develops. The contact angle formed between the surfaces treated with  $\text{TiO}_2$  and water drops is close to  $1^\circ$ . This phenomenon causes the water to spread and wet the surface, creating a nanometer-sized film, which is durable for two days after irradiation of the surface with UV light. This irradiation leads to the formation of oxidative agents able to decompose organic and inorganic materials, increasing the self-cleaning

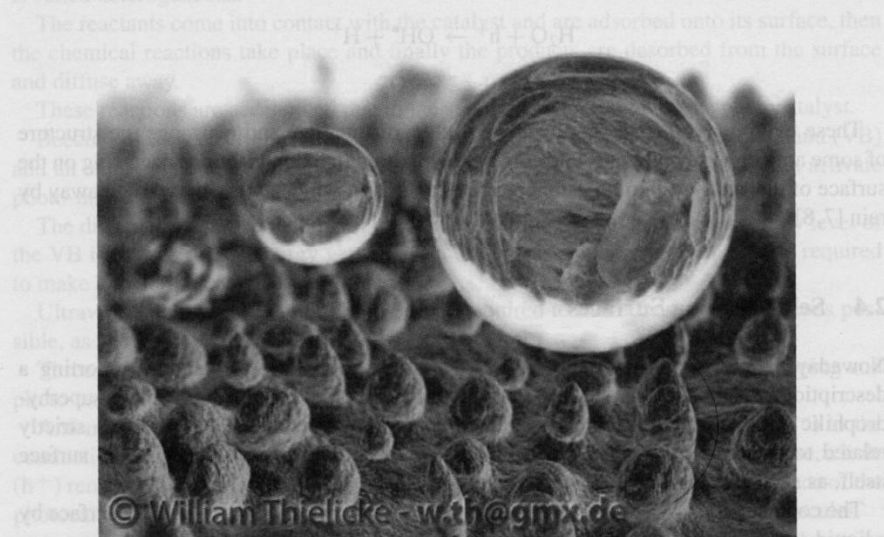


**Figure 2.3** Computer graphic of lotus leaf surface. Source: Image courtesy of W. Thielicke, <http://wthielicke.gmxhome.de/> last accessed 15/01/2013.



property. This sheeting action not only helps rinse away loosened dirt and other organic material but also minimizes spots and streaks by helping the surface dry more quickly and uniformly.

Main applications of this property are the development of nanometric  $\text{TiO}_2$  films for glass substrates (e.g. driving mirrors, highway sound barriers, solar cell cover glass, etc.)

Focusing our interest on the construction industry, many experimental studies demonstrate the efficiency of photocatalytic cementitious products made with titanium dioxide and cement [9], depending upon the formulation used, in terms of:

- Self-cleaning property: the capability to favour the removal of most organic and some inorganic pollutants that deposit on cementitious surfaces, causing stains and discoloration;
- Pollution reduction: the capability to remove significant amounts of environmental pollutants deemed harmful to human health.

#### 2.4.1 Mechanisms of Photo-Reduction of Air Pollutants

When air pollutants (e.g.  $\text{NO}_x$ ,  $\text{SO}_x$ , VOC and particulate matter) come into contact with a photocatalytic surface containing titanium dioxide, they undergo a process of absorption, decomposition and final transformation into limestone and mineral salts which can be easily washed away by rain. Organic pollutants are thus degraded with the formation of  $\text{CO}_2$ .

These photocatalytic reactions take place on a titanium dioxide surface and have a multi-phasic character, both at  $\text{TiO}_2$ /water and  $\text{TiO}_2$ /air interfaces.

Photochemical degradation of air pollutants is a consequence of the decomposition of oxygen and water on surfaces treated with  $\text{TiO}_2$  and the formation of hydroxyl radicals and highly reactive superoxide ions.

As a result of the photocatalytic oxidation, all elements presenting in a molecule of air pollutant are mineralized to inorganic species: carbon to  $\text{CO}_2$ , hydrogen to  $\text{H}_2\text{O}$ , halogens to halide ions, sulfur to sulfates, and phosphorus to phosphates, respectively.

Several researches document the breaking up of the dioxin benzene ring by OH radicals, produced by photo-oxidation of water [10].

The decomposition of nitrogen oxide in air takes place through oxidation under ultraviolet light to nitric acid,  $\text{HNO}_3$ , and partially to nitrogen dioxide,  $\text{NO}_2$ . When  $\text{NO}_2$  is formed, part of the gas may escape from the photocatalytic surface, but in the presence of a cementitious matrix the gas may be effectively trapped together with the nitric acid formed, and can be easily removed from the surface by atmospheric water [11–13].

The system obtained by mixing  $\text{TiO}_2$  with cement well creates the conditions for environmental photocatalysis. Most of the photo-oxidizing compounds, including  $\text{NO}_2$  and  $\text{SO}_2$ , are acidic. The basic nature of the cement matrix fixes both the polluting reagent and the photo-oxidation products on its surface.

#### 2.4.2 Some Experimental Evidences

In recent years many research programs have started in this field, motivated by the growing interest and multiple applications of photocatalytic materials; one of these was the "Photocatalytic Innovative Coverings Applications for Depollution Assessment" (PICADA) project.



**Figure 2.4** The canyon street pilot ([www.picada-projet.com](http://www.picada-projet.com)). Source: Reproduced by permission of C.T.G. S.p.A.

This research program started in 2002 and ended in 2005, with the participation of the European Community, four industrial partners and some European research centres, for a total investment of €3.4 million.

The aim of the project was to develop a range of photocatalytic covering materials and to evaluate their effect on a large scale, typically in street canyons, to better understand the photocatalytic reaction mechanisms and their effect on cleaning and de-pollution.

The project was divided into eight work-packages focusing on the improvement of material properties, pre-development of applications and drafting guidelines.

A wide range of mineral and organic coatings was selected for testing, in different thickness and with added nano-sized  $\text{TiO}_2$ .

Several laboratory procedures were elaborated and some of these were codified by the Italian Standardisation Organisation (UNI) and are described in the next section.

Further experience of a canyon street pilot (Figure 2.4), simulating an urban environment, was realized monitoring  $\text{NO}_x$  and  $\text{O}_3$  with chemiluminescence analyzers.

The difference between the  $\text{NO}_x$  levels in the canyons indicated the significant capability of photocatalytic coatings to remove  $\text{NO}_x$  from the air.  $\text{NO}_x$  recorded concentrations in treated surfaces were 40 to 80% lower than those observed in the untreated reference canyon.

Cassar evaluated the behaviour of different nano-sized  $\text{TiO}_2$ , showing no direct correlation between increasing the specific surface area of the photocatalyst and the photocatalytic activity of the  $\text{TiO}_2$ /cement system. Laboratory tests showed a better efficiency of 150 nm  $\text{TiO}_2$  particles with respect to 15–20 nm ones, in the degradation of two different dyes, Rhodamine B and Bromocresol Green; thus on decreasing the specific surface area, the photocatalytic activity increased by about 10%. Moreover, mixing different particle sizes of photocatalyst gives a synergic effect, providing the best efficiency with a mixture of different particle sizes of  $\text{TiO}_2$  [14].

Cassar *et al.* tested the efficiency towards photo-degradation of unsaturated hydrocarbons and polycondensate aromatic compounds from tobacco cigarette ash by cementitious mortars with added  $\text{TiO}_2$  (1–2%) [15].

Diamanti *et al.* evaluated the photocatalytic activity of fiber-reinforced mortars based on white cement and titanium dioxide, in terms of the photo-degradation of 2-propanol, a

model reactant of VOC present in the atmosphere, to acetone and water by UV irradiation. The best results were achieved by spreading 2%  $\text{TiO}_2$  aqueous suspension on the surface samples so as to form a nanometric layer, improving the wettability of the envelope. On the other hand, samples with 3%  $\text{TiO}_2$  added and mixed with cement showed the best results in terms of maintenance of colour after exposure to outdoor urban environments [16].

Because of the activation of  $\text{TiO}_2$  dispersed in a cementitious matrix, strictly related to the UV light, and because of the wide use of colour in the building envelope by designers and architects, the influence of the addition of mineral pigments on the photocatalytic and depolluting performances of finishing products was evaluated.

Mineral pigments were added in amounts from 0.1 to 0.5% to provide a significant coloration of surfaces and revealed a moderate decrease in the photocatalytic activity, in terms of  $\text{NO}_x$  abatement, evaluated through the procedure of the UNI 11247:2010, described in the following section.

The analysis was focused on three different building products: plasters, finishing coatings and paints, setting the samples in different ageing conditions (inside laboratory and outdoor conditions).

The tested pigments were yellow, brown, red, blue and green, dry added to the binder mixtures. Preliminary tests were made on them using absorption spectrophotometry to evaluate the absorption spectrum.

Even the lighter colours, such as yellow and red, absorbing the light radiation from near-ultraviolet wavelengths, decreased the overall absorption of light radiation of wavelength  $\lambda < 410$  nm in the mortars, thus lowering the photocatalytic activity (Figure 2.5).

External ageing reduced the degradation of nitrogen dioxides more than under laboratory conditions (Figure 2.6). The least reduction was found with the brown pigment and among others, paint was the most effective.

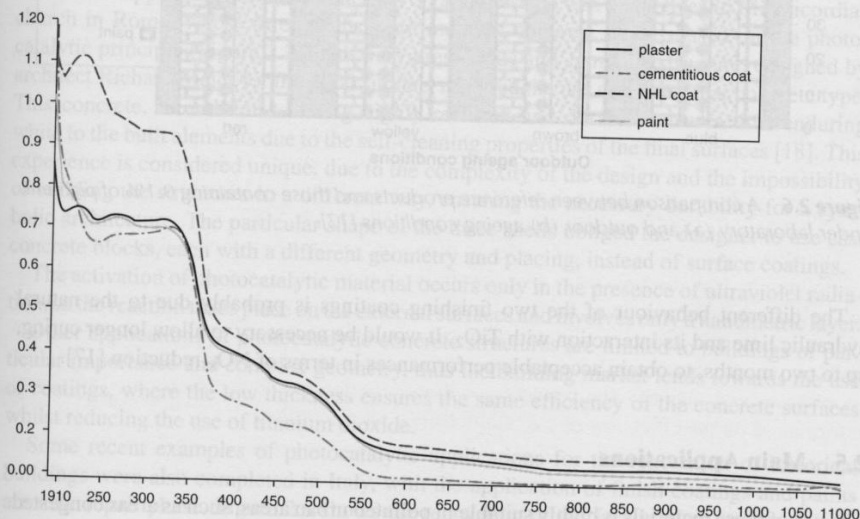
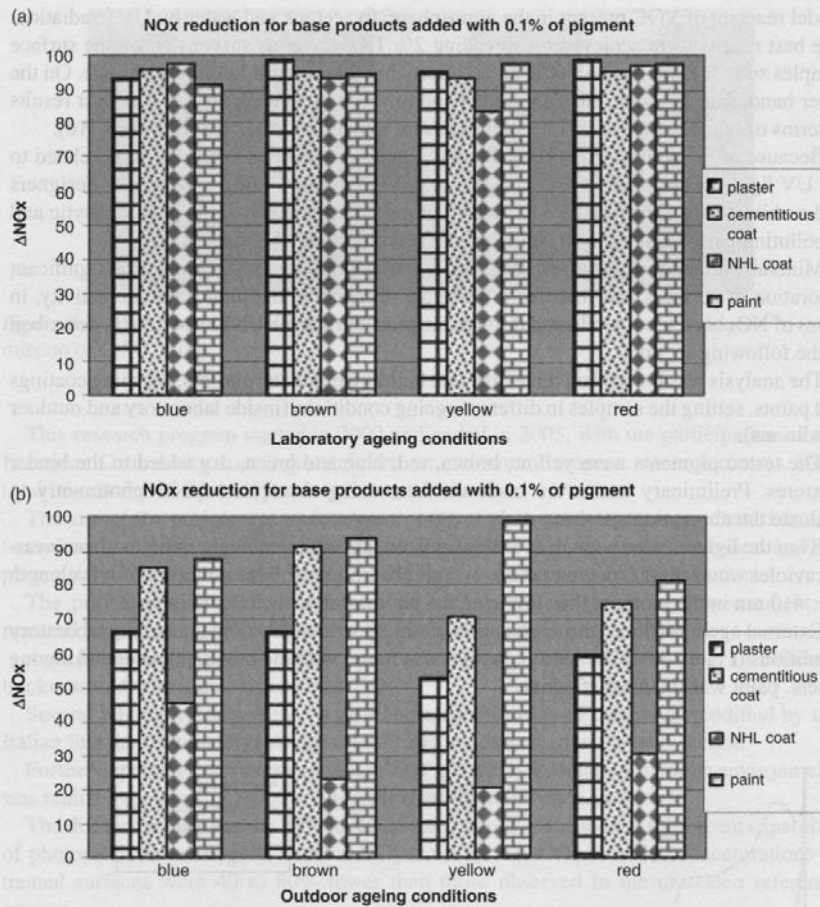


Figure 2.5 Absorption spectra of outdoor aged samples with 0.1% yellow pigment.



**Figure 2.6** A comparison between reference products and those containing 0.1% of pigment, under laboratory (a) and outdoor (b) ageing conditions [17].

The different behaviour of the two finishing coatings is probably due to the natural hydraulic lime and its interaction with TiO<sub>2</sub>. It would be necessary to allow longer curing, up to two months, to obtain acceptable performances in terms of NO<sub>x</sub> reduction [17].

## 2.5 Main Applications

The use of these materials is highly suitable in polluted urban areas, such as areas congested by vehicular traffic, tunnels and historical centres of the city, where narrow streets cannot

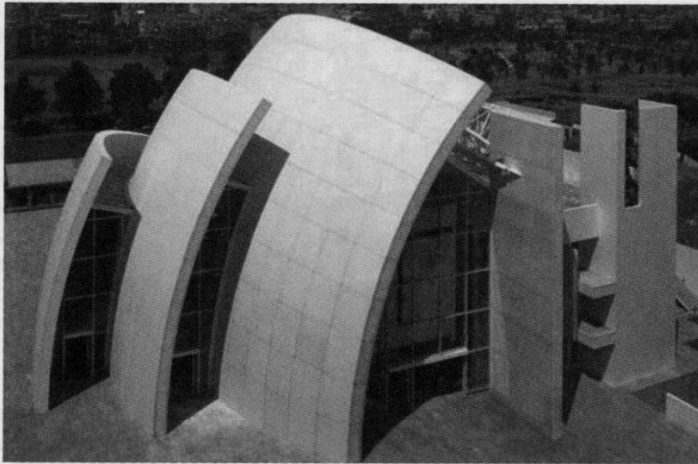


**Figure 2.7** The three shells of the Dives in the Misericordia church in Rome [13]. Source: Reproduced by permission of C.T.G. S.p.A.

be easily closed to traffic. Moreover, using these materials increases the durability and facilitates the maintenance of external surfaces.

The building market provides a wide range of photocatalytic building materials: coatings, such as plasters, paints, tiles and asphalt pavements, and also structural materials, such as pavement blocks and concrete.

The first application of these materials on a large scale was the “Dives in Misericordia” church in Rome, whose three shells were made of concrete blocks based on the photocatalytic principle (Figure 2.7). This very prestigious and symbolic structure, designed by architect Richard Meier for the 2000 Jubilee, required the use of a particular concrete type. This concrete, in addition to being highly resistant and durable, ensures time-enduring white to the built elements due to the self-cleaning properties of the final surfaces [18]. This experience is considered unique, due to the complexity of the design and the impossibility of building the structures in a different way, ensuring the necessary durability for a symbolic architecture. The particular shape of the three shells obliged the designer to use cast concrete blocks, each with a different geometry and placing, instead of surface coatings.

The activation of photocatalytic material occurs only in the presence of ultraviolet radiation, so the reaction takes place on the external surfaces and involves only a nanometric layer.

Other applications of photocatalytic concrete structures are limited to buildings of particular importance and complex geometry, thus the building market tends towards the use of coatings, where the low thickness ensures the same efficiency of the concrete surfaces whilst reducing the use of titanium dioxide.

Some recent examples of photocatalytic applications for the renovation of historical buildings were also completed in Italy, with the application of finish coatings and paints after the repair phase. Figure 2.8 shows the renovation of the facade of an Italian church, where photocatalytic paint was applied. The worthiness of the monument, made of historical





**Figure 2.8** The facade of the Matrice church in Cittanova (RC) ([www.nonsolocittanova.it](http://www.nonsolocittanova.it)). Source: Image courtesy of A. Mesiti, Cittanova (RC), [www.nonsolocittanova.it](http://www.nonsolocittanova.it).

masonry, and the necessity to preserve the original plaster led to the choice of a coating product based on natural hydraulic lime with a low content of cement as being more suitable for this intervention.

## 2.6 Test Methods

As mentioned before, there is no worldwide standard to evaluate the self-cleaning effect, but there are many standards to evaluate other parameters strictly related to this property. One of these parameters is colour, the durability of which is influenced by the capability of surfaces to remain clean.

The Italian Standardisation Organisation (UNI) in recent years has published three standards dealing with the photocatalytic activity of cement-based materials to evaluate the capability of these materials to degrade air pollutants (NO<sub>x</sub> test, UNI 11247:2009; BTEX test, UNI 11238-1:2007 and Rhodamine B test, UNI 11259:2008).

The above mentioned standards refer to direct procedures to measure the abatement of air pollutants. Nonetheless, there are other indirect approaches, not codified by standards, to evaluate the photocatalytic activity. Among others, X-ray photoelectron spectroscopy (XPS) and Raman spectroscopy are suitable to investigate the external nanolayers of the building envelope where photocatalytic reactions take place. These techniques are able to evaluate and quantify the products of the air pollutants degradation, thus providing information on the efficiency of the photocatalyst on the surface.

### 2.6.1 Colour

Monitoring the colour of a surface helps to evaluate the efficiency in terms of maintaining surfaces clean, as a result of the presence of a photocatalyst.

The UNI EN ISO 3668:2002 deals with the visual comparison of paints and varnishes commonly used in the paint and related coatings industry. The tolerances and differences are expressed in terms of approximately uniform visual colour perception in the CIE 1976 ( $L^* a^* b^*$ ) colour space, well known as CIELAB colour space, and other colour spaces.

CIELAB is an approximately uniform colour space based on nonlinear expansion of the tristimulus values and takes differences to produce three axes that approximate the perception of lightness–darkness ( $L^*$  axis), redness–greenness ( $a^*$  axis) and yellowness–blueness ( $b^*$  axis).

CIELAB colour space was designed by the International Commission on Illumination (CIE means Commission Internationale de l'Éclairage) to approximate human vision.

The total colour difference,  $\Delta E_{ab}^*$ , between two colours, is a parameter calculated by the measurement of  $L^*$ ,  $a^*$ ,  $b^*$  and is given by the formula:

$$\Delta E_{ab}^* = \sqrt{(\Delta L^*)^2 + (\Delta a^*)^2 + (\Delta b^*)^2}$$

The magnitude,  $\Delta E_{ab}^*$ , gives no indication of the character of the difference since it does not indicate the relative quantity and direction of hue, chroma, and lightness differences. The direction of the colour difference is described by the magnitude and algebraic signs of the components  $\Delta L^*$  (positive means lighter, negative means darker),  $\Delta a^*$  (positive = redder, negative = greener) and  $\Delta b^*$  (positive = yellower, negative = bluer).

The classification proposed is a scale of the colour difference  $\Delta E_{ab}^*$  starting from zero, that means no perceptible difference, to five representing very significant difference.

This classification does not account for the different colour perception by the human eye that is more sensitive to some colours than others. Therefore, within the visible spectrum, the colour difference,  $\Delta E_{ab}^*$ , can be perceptible or insignificant to the human eye, depending on the spectrum area considered.

The concept of Just Noticeable Difference (JND) was defined for this reason, in which the acronym means the hardly noticeable colour difference to the human eye. In the CIE 1931 colour space, MacAdam, in the 1940s, defined some ellipses in the  $xy$  chromaticity diagram, being the brightness constant, the contours of which (Figure 2.9) vary in size and tolerance and represent the JND of chromaticity [19].

An assessment of JND, although quite approximate, was conducted by Sharma [20], defining the value of  $\Delta E_{ab}^*$  of about 2.3 as the limit for the colour difference perceptible to the human eye.

A similar treatment was carried out for the Cité de la Musique and Beaux Arts building in Chambéry (Figure 2.10), in the south of France, close to the Italian border, between 1999 and 2001, of pre-cast concrete structural elements, based on the photocatalytic principle. The monitoring of the colour of its grey elements was carried out after three years from the completion and the results were a medium colour difference, in the four facades that were differently oriented, lower than 1 point [21].

## 2.6.2 Photocatalytic Degradation of Nitrogen Oxides

The UNI 11247:2010 standard deals with the determination of the catalytic degradation of nitrogen oxides in air by photocatalytic inorganic materials (cementitious and ceramic materials). The tests are carried out on samples set inside a reaction chamber, coming into contact with a continuous gas flow of  $3 \text{ l min}^{-1}$ , with fixed  $\text{NO}_x$  concentration (equal to

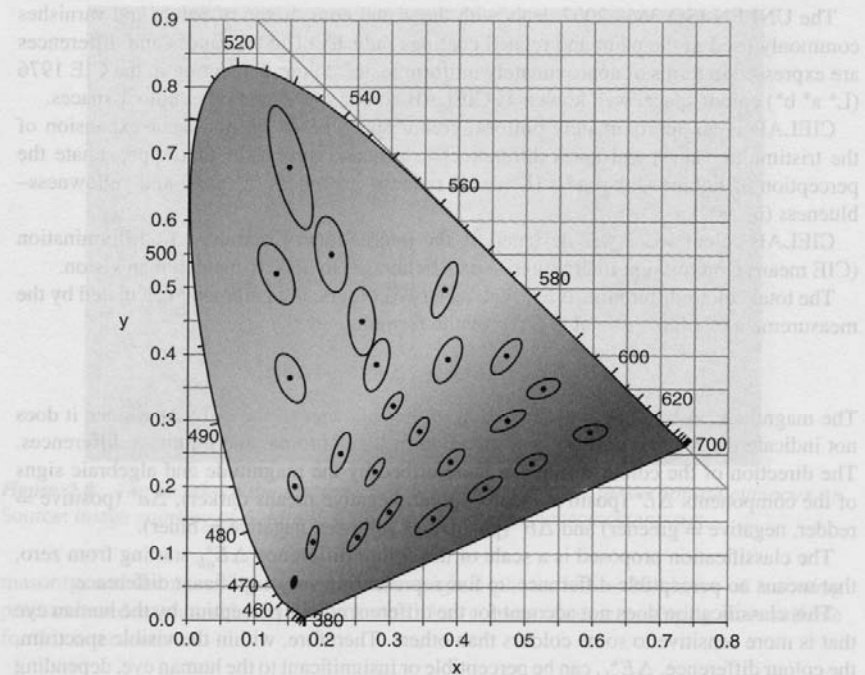


**Figure 2.9** Standard deviations of chromaticity from indicated standards on CIE 1931 standard chromaticity diagram (Creative Commons Attribution-Share Alike 3.0 Unported licence).



**Figure 2.10** The Cité de la Musique and Beaux Arts building in Chambéry [22]. Source: Reproduced by permission of C.T.G. S.p.A.

0.55 ppm, of which 0.15 ppm is NO<sub>2</sub> and 0.4 ppm NO) in N<sub>2</sub>, corresponding to a possible atmospheric pollution. The results can be expressed as a percentage of NO<sub>x</sub> decomposition by a photocatalytic sample under UV radiation, supplied by a UV lamp, 300 W power and irradiance at 365 nm, providing a light intensity of  $20 \pm 1 \text{ W m}^{-2}$ .

The concentration of NO<sub>x</sub> inside the reaction chamber is measured with a chemiluminescence NO<sub>x</sub> meter in two different phases: the first one is in the dark and measurements are taken after 30 and 60 min with the UV lamp switched off. In the second phase, with the UV lamp on, measurements are taken after 30 and 60 min, when the concentrations have reached equilibrium.

The photocatalytic activity ( $A_F$ ) in terms of nitrogen oxides degradation is calculated by the formula:

$$A_F = \frac{(C_B - C_L)FI}{C_B S}$$

Where:

$C_B$  is the concentration of NO<sub>x</sub> in dark conditions, at equilibrium ( $\mu\text{g m}^{-3}$ )

$C_L$  is the concentration of NO<sub>x</sub> in light conditions, at equilibrium ( $\mu\text{g m}^{-3}$ )

$F$  is the gas flow ( $\text{m}^3 \text{h}^{-1}$ )

$S$  is the geometrical surface area of the sample ( $\text{m}^2$ )

$I$  is the adimensional intensity of the luminous flow, obtained by the ratio of the experimentally measured intensity  $I'$  ( $\text{W m}^{-2}$ ) and  $1000 \text{ W m}^{-2}$ , corresponding to about 100.000 Lux, the average value of sunlight at noon on an average July day in Italy.

The photocatalytic activity of nitrogen oxides degradation can also be calculated as the percentage reduction of the nitrogen oxides –  $\Delta\text{NO}_x$  – equal to the difference between the measured concentrations of NO, NO<sub>x</sub> and NO<sub>2</sub> in dark,  $C_B$ , and light conditions,  $C_L$ .

$$\Delta\text{NO}_x = 100 \frac{(C_B - C_L)}{C_B} \%$$

The test set-up is represented in Figure 2.11.

### 2.6.3 Photocatalytic Degradation of Micro-Pollutants in Air

The UNI 11238-1:2007 standard is referred to photocatalytic cementitious materials and deals with the determination of the photocatalytic degradation of organic micro-pollutants present in the atmosphere particularly all those included in the acronym BTEX (benzene, toluene, ethylbenzene and xylenes). These organic pollutants are some of the volatile organic compounds (VOCs) present in petroleum derivatives such as gasoline and diesel fuel. Using this standard, it is possible to measure the degradation of several compounds of a standardized mixture of BTEX promoted by photocatalytic cementitious materials, under an irradiance of  $1000 \mu\text{W cm}^{-2}$  in the UV-A spectral band.

The test procedure is based on the measurement of the equilibrium concentration of every component of the BTEX mixture inside a photo-chemical reactor where the sample is set, with a constant gaseous stream of a mixture of air and BTEX. These equilibrium concentrations are measured with the UV-A light source switched on and off. The

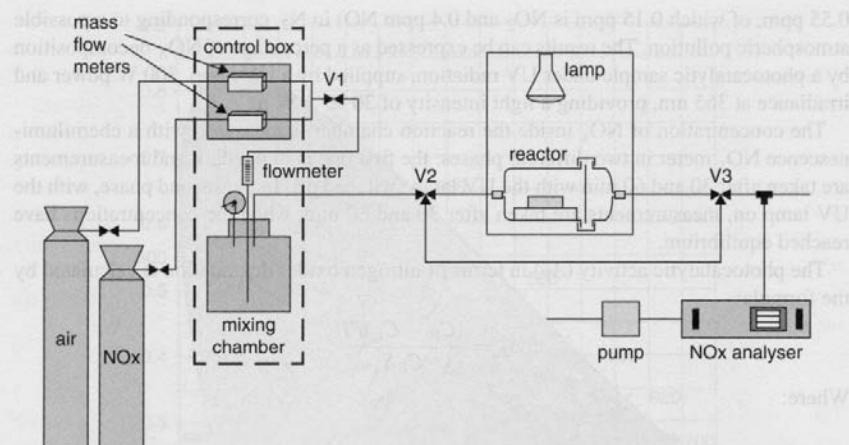


**Figure 2.11** Operational scheme of the test of photocatalytic activity (UNI 11247:2010). Source: Reproduced by permission of C.T.G. S.p.A.

photocatalytic activity of the sample is then determined as a function of the concentration of the compound, the mixture flow, the irradiance in the UV-A spectral band and the surface area of the sample. The result is expressed for every component of the BTEX in terms of photocatalytic activity measured in  $(\mu\text{g m}^{-2} \text{h}^{-1})/(\mu\text{g m}^{-3})$  or in  $\text{m h}^{-1}$ .

The standard defines two different BTEX mixtures, at low and high concentration, as in Table 2.1, and the pollutant concentrations in the gaseous stream and the irradiation levels are comparable to those found in real ambient conditions.

The temperature has to be constant at  $23^\circ\text{C}$  during the entire test, the gaseous stream has to ensure  $3 \pm 0.5$  air changes per hour and a gas chromatography analyser has to analyse and measure the concentrations of the organic compounds, before and after contact with photocatalytic surface of the sample set inside the photochemical reactor.

The dimensions of the sample are related to the volume of the photochemical reactor and the ratio is  $3 \pm 1 \text{ m}^2/\text{m}^3$ , the thickness has to be between 3 and 20 mm.

**Table 2.1** Pollutants concentrations of the two mixtures used in the test.

Component	BTEX low concentration mixture	BTEX high concentration mixture
Nitrogen	$79 \pm 1\%$	$79 \pm 1\%$
Oxygen	$21 \pm 1\%$	$21 \pm 1\%$
Relative humidity	$10.3 \pm 0.5 \text{ g m}^{-3}$	$10.3 \pm 0.5 \text{ g m}^{-3}$
Benzene	$100 \pm 10 \text{ ppb}$	$300 \pm 30 \text{ ppb}$
Toluene	$100 \pm 10 \text{ ppb}$	$300 \pm 30 \text{ ppb}$
Ethylbenzene	$100 \pm 10 \text{ ppb}$	$300 \pm 30 \text{ ppb}$
Xylenes	$100 \pm 10 \text{ ppb}$	$300 \pm 30 \text{ ppb}$



The test has two different stages; in the first, the concentrations of organic compounds are measured in dark conditions, after 24 h of direct contact of the gaseous mixture flow with the surface of the sample, until equilibrium is reached.

Then, the circuit is closed and the sample irradiated with the UV-A lamp for 24 h at least. The concentrations of all BTEX are measured at equilibrium, confirmed after a measurement after 12 h. The photocatalytic activity ( $A_{CAT}$ ) of the sample is calculated through the following formula:

$$A_{CAT} = \frac{1000(C_{ALIM} - C_{IRRAD})F}{IAC_{IRRAD}} \text{ m h}^{-1}$$

Where:

$C_{ALIM}$  is the initial concentration of each organic compound of BTEX at equilibrium ( $\mu\text{g m}^{-3}$ )

$C_{IRRAD}$  is the concentration of each organic compound of BTEX at equilibrium during the irradiation phase ( $\mu\text{g m}^{-3}$ )

$F$  is the gas flow ( $\text{m}^3 \text{h}^{-1}$ )

$A$  is the geometrical surface area of the sample ( $\text{m}^2$ )

$I$  is the irradiance on the surface of the sample at the UV-A spectral band ( $\mu\text{W cm}^{-2}$ )

The UNI 11238-2:2007 standard is referred to photocatalytic ceramic materials and is very similar to the Part 1 of the standard, dealing with the determination of the photocatalytic degradation of BTEX.

#### 2.6.4 Photocatalytic Degradation of Rhodamine B

Rhodamine B is a red fluorescent dye, which is used in the UNI 11259:2008 test to evaluate the photocatalytic activity of hydraulic binders. This is a colorimetric method and measurements are referred to CIELAB colour space, particularly to the  $a^*$  coordinate, which represents the colorimetric axis with red and green in opposition.

The concentration of the Rhodamine B in distilled water has to be  $0.05 \pm 0.005 \text{ g l}^{-1}$  and the minimum value of hydraulic binder  $a^*$  is 12.

The test lasts for 26 h and is based on the measure of the evolution of the  $a^*$  coordinate of a cementitious sample treated with Rhodamine B, under UV light, ensuring an irradiance equal to  $3.75 \pm 0.25 \text{ W m}^{-2}$ .

The sample has a standard composition and each mixture contains  $450 \pm 2 \text{ g}$  of hydraulic binder,  $1350 \pm 5 \text{ g}$  of normalised sand and  $225 \pm 1 \text{ g}$  of water so as to keep the water/cement ratio at 0.50.

Mixing has to be at two different rates, a low rate of  $140 \pm 5$  revolutions per  $\text{min}^{-1}$  for 60 s after adding water to the binder and 30 s at a high rate of  $285 \pm 10$  revolutions per  $\text{min}^{-1}$ . After a 90 s stop, the revolutions have to restart for 60 s at the high rate.

Sample dimensions are  $16 \times 14 \times 4 \text{ cm}^3$  with 0.5 cm tolerance and each test deals with four samples with the same concentration.

Sample aging takes place in water at  $20 \pm 1^\circ\text{C}$  for 7 days and in atmospheric air for a further 7 days.

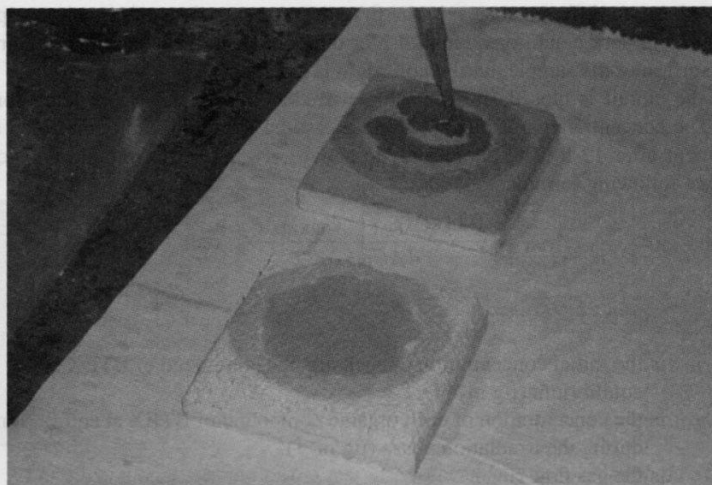


**Figure 2.12** The application of Rhodamine B to the samples.

All the surface of the samples, except the centre part, has to be covered with a hydrophobic material, silicone preferably, so as to mark off a central area of  $22 \pm 2 \text{ cm}^2$ . Then the untreated area has to be wet with the Rhodamine B 0.5 ml solution (Figure 2.12) and set in dark conditions for 24 h at  $20 \pm 1^\circ\text{C}$  and  $60 \pm 10\%$  RH.

The first measurement,  $a^*(0)$ , as an average of three measurements on the circular area, has to be taken with a colorimeter or a spectrophotometer, the second after 4 h,  $a^*(4)$ , and the final one after 26 h,  $a^*(26)$ .

The result is the average of the measurements taken on three samples; the values obtained should be within 10% of each other, otherwise the sample has to be discarded and the fourth sample is considered.

The sample can be considered photocatalytic with respect to the Rhodamine B, if the results satisfy the following:

$$R_4 > 20\%$$

$$R_{26} > 50\%$$

where:

$$R_4 = 100 \frac{a^*(0) - a^*(4)}{a^*(0)} \%$$

$$R_{26} = 100 \frac{a^*(0) - a^*(26)}{a^*(0)} \%$$

Recent studies showed a possible interaction with other organic admixtures in the products impacting the efficiency of this method to evaluate the photocatalytic activity of hydraulic binders.

### 2.6.5 Spectroscopic Techniques

X-ray photoelectron spectroscopy can provide information on the electronic structure and atomic quantitative analysis in the top 5 nm of the surface. It is based on X-rays, of energy  $h\nu$ , exciting electrons from the valence band of surface atoms which are then ejected. The kinetic energy of these photoelectrons is measured by an electron energy analyser and the binding energy of the photoelectron can be calculated by this measured energy and the intrinsic characteristic of the spectrometer. The calculated peaks are easily identified using tabulated binding energy values from XPS handbooks, yielding information on chemical composition and bonding environments.

Raman spectroscopy provides information on both the crystal structure and bonding characteristics of matter. It is based on inelastic scattering of monochromatic light, usually from a laser in the visible, near-infrared or near-ultraviolet range. The energy difference between the incident and reflected beam corresponds to a change in molecular vibration. These characteristic bond vibrations allow chemical and crystal state identification of matter.

Particularly, Dalton *et al.* used these two techniques to evaluate the photocatalytic oxidation of  $\text{NO}_x$  gases promoted by a  $\text{TiO}_2$ -treated surface, under UV irradiation. The XPS technique was applied to differentiate and quantitatively measure the adsorbed nitrogen species, such as  $\text{NH}_3$ ,  $\text{NO}$ ,  $\text{NO}_2$  and  $\text{NO}_3^-$ . Raman spectroscopy was used to characterize the chemical bonds of the adsorbed atoms and molecules. They showed the mechanism of  $\text{NO}_x$  removal based on its degradation into harmless nitrates adsorbed on the  $\text{TiO}_2$  surface [23].

A similar technique is molecular absorption spectroscopy in the ultraviolet (UV) and visible (VIS) which measures the absorption of radiation in its passage through a gas, a liquid or a solid. The wavelength region generally used is from 190 to about 1000 nm and the result of the absorption of photons of energy in this range of wavelengths is an absorption spectrum. Through this technique it is possible to provide two different analyses: qualitative and quantitative. The qualitative method leads to the identification of an analyte by comparing the absorption spectrum of the unknown substance with spectra of known substances. The quantitative method is based on the relation between absorbed radiation intensity and concentration. A known analyte can be determined by measuring the absorbance at one or more wavelengths and using the Beer–Lambert law and the molar absorption coefficient to calculate its amount concentration.

Comparelli *et al.* monitored the photodegradation of Methyl Red, an organic dye, promoted by  $\text{TiO}_2$ -based photocatalysts. Due to its nature as a pH indicator, being red for pH less than 4.2 and yellowing with pH greater than 6.2, Methyl Red has an absorption spectrum depending on pH, so UV/VIS absorption spectroscopy was used [24].

Rashed *et al.* used the same method to evaluate and monitor the photocatalytic degradation of Methyl Orange in a solution of  $\text{TiO}_2$  [25].

## 2.7 Future Developments

The application of photocatalytic materials is continuously increasing in building construction. Several technologies are being developed to improve the efficiency of  $\text{TiO}_2$  and other photocatalysts as depolluting agents for superficial applications.

Japanese researchers are studying the possibility to realize an energy saving cooling method by covering the external walls of a building with titanium dioxide film [26].

The improvement in photocatalytic technologies is focusing on responding to society's needs: environmental protection, enhanced aesthetic value and durability of buildings.

In terms of air pollution, researchers aim at increasing the decomposition properties of photocatalytic surfaces towards nitrogen and sulfur oxides.

Great interest is arising in photocatalytic road surfaces and technologies to reduce the impact and the negative effect of particulate and powder, together with the development of systems able to measure *in situ* the reduction in air pollutants [27].

Hunger *et al.* developed a laboratory set-up to assess the decomposition of  $\text{NO}_x$  promoted by concrete paving stones and derived a reaction model to predict quantitatively the efficiency in air-purifying of these concrete materials [28].

The efficiency of bituminous pavements was also studied by Da Rios *et al.* through laboratory tests on cementitious photocatalytic mortar applied on an open graded bituminous layer. Photocatalytic activity was evaluated in terms of nitrogen dioxides abatement with the equipment described in the UNI 11247:2010 and results confirm efficiency up to 40%. The elaboration of a mathematical model to simulate the  $\text{NO}_x$  degradation mechanisms was conducted [29].

The Italian research group at Palermo is beginning a research program with the C.T.G. S.r.l., the research and development branch of the Italcementi group, and Hydratite, the local industrial partner, entitled "Assessment of the durability of photocatalytic cementitious materials aimed at the maintenance scheduling and planning" and coordinated by Prof. G. Alaimo. This program, following the methodology of the ISO 15686 and the UNI 11156:2006, aims to assess the durability of plasters, coatings and paints, in terms of photocatalytic activity, expressed by  $\text{NO}_x$  reduction, maintenance of colour, resistance to saline aggressive atmospheres and resistance to abrasion of surfaces. The methodology foresees the exposure of samples to natural environment and artificial conditions produced by a climatic chamber (temperature range of 0 to 80 °C, relative humidity range 0 to 100%, rain and UV irradiation) and the comparison of results to make a hypothesis on the rescaling of laboratory and outdoor parameters decay.

## References

1. Fujishima, A. and Honda, K. (1972) Electrochemical photolysis of water at a semiconductor electrode. *Nature*, **238**, 37–38.
2. Forastiere, F., Peters, A., Kelly, F.J. and Holgate, S.T. (2005) Nitrogen dioxide, in *Air Quality Guidelines: Global Update 2005, Particulate Matter, Ozone, Nitrogen Dioxide and Sulphur Dioxide*, World Health Organization Europe.
3. Samet, J.M., Brauer, M. and Schlesinger, R. (2005) Particulate matter, in *Air Quality Guidelines: Global Update 2005, Particulate Matter, Ozone, Nitrogen Dioxide and Sulphur Dioxide*, World Health Organization Europe.
4. Harrison, R.M. (2005) Source of air pollution, in *Air Quality Guidelines: Global Update 2005, Particulate Matter, Ozone, Nitrogen Dioxide and Sulphur Dioxide*, World Health Organization Europe.



5. (2003) Chemical Sampling Information: Benzene, Occupational Safety and Health Administration, United States Department of Labor.
6. Rothenberg, G. (2008) *Catalysis: Concepts and Green Applications*, Wiley-VCH, Weinheim.
7. Linsebigler, A.L., Lu, G. and Yates, J.T. (1995) Photocatalysis on TiO<sub>2</sub> surfaces: principles, mechanisms, and selected results. *Chem. Rev.*, **95**, 735–758.
8. Hashimoto, K., Irie, H. and Fujishima, A. (2007) TiO<sub>2</sub> photocatalysis: a historical overview and future prospects. *AAPPS Bull.*, **17** (6), 12–28.
9. Cassar, L., Beeldens, A., Pimpinelli, N. and Guerrini, G.L. (2007) Photocatalysis of cementitious materials, RILEM Int. Symposium on Photocatalysis, Environment and Construction Materials, Florence, RILEM PRO 55, pp. 131–145.
10. Choi, W. (2006) Pure and modified TiO<sub>2</sub> photocatalysts and their environmental applications. *Catal. Surv. Asia*, **10**(1), 16–28.
11. Yumoto, H., Matsudoa, S. and Akashib, K. (2002) Photocatalytic decomposition of NO<sub>2</sub> on TiO<sub>2</sub> films prepared by arc ion plating. *Vacuum*, **65** (3–4), 509–514.
12. Ibusuki, T. and Takeuchi, K. (1994) Removal of low concentration nitrogen oxides through photoassisted heterogeneous catalysis. *J. Mol. Catal.*, **88** (1), 93–102.
13. Cassar, L. (May 2004) Photocatalysis of cementitious materials: clean buildings and clean air. *Mater. Res. Soc. Bull.*, **29**, 328–331.
14. Cassar, L. (2005) Nanotechnology and photocatalysis in cementitious materials. Proceedings of NICOM'2, Bilbao, November 2005.
15. Cassar, L., Pepe, C., Pimpinelli, N. *et al.* (1997) *Materiali Cementizi e Fotocatalisi*, FAST, Milan.
16. Diamanti, M.V., Ormellese, M. and Pedferri, M.P. (2008) Characterization of photocatalytic and superhydrophilic properties of mortars containing titanium dioxide. *Cement Concrete Res.*, **38**, 1349–1353.
17. Enea, D. and Guerrini, G.L. (2010) Photocatalytic properties of cement-based plasters and paints containing mineral pigments. *J. Transport. Res. Board*, **2141**, 52–60.
18. Cassar, L., Pepe, C., Tognon, G. *et al.* (2003) White cement for architectural concrete, possessing photocatalytic properties. Proceedings of the 11th Int. Congress on the Chemistry of Cement, Durban, South Africa, Vol. 4, pp. 2012.
19. MacAdam, D.L. (1942) Visual sensitivities to color differences in daylight. *J. Opt. Soc. Am.*, **32** (5), 247–274.
20. Sharma, G. (2003) *Digital Color Imaging Handbook*, CRC Press.
21. Guerrini, G.L. and Guillot, L. (2006) Realizzazione di edifici con utilizzo di cementi fotocatalitici. *Proceedings of the 16th congress C.T.E., Parma*, Vol. **2**, pp. 941–950.
22. Chiesa, G., Elias, G., Franchi, A. and Migliacci, A. (2009) Vademecum della progettazione consapevole, in *Costruire per la qualità della vita: Expo 2015 un'occasione concreta*, FAST, Milan.
23. Dalton, J.S., Janes, P.A., Jones, N.G. *et al.* (2002) Photocatalytic oxidation of NO<sub>x</sub> gases using TiO<sub>2</sub>: a surface spectroscopic approach. *Environ. Pollut.*, **120**, 415–422.
24. Comparelli, R., Cozzoli, P.D., Curri, M.L. *et al.* (2004) Photocatalytic degradation of methyl-red by immobilized nanoparticles of TiO<sub>2</sub> and ZnO. *Water Sci. Technol.*, **49**, 183–188.







# Self-Cleaning Materials and Surfaces

## A Nanotechnology Approach

**Editor: Walid A. Daoud**


*School of Energy and Environment, City University of Hong Kong, Hong Kong*

**INSPIRED BY** the structure of a lotus leaf, self-cleaning surfaces are based on the hydrophobic effect, which causes water droplets to roll off, carrying away dirt and debris. Similar microstructures exist on butterfly wings, and moth eyes. Hydrophilic self-cleaning, also known as the photocatalytic effect, uses photoactive substances to decompose dirt and pollutants under light exposure. Hydrophilic self-cleaning materials offer additional properties such as antimicrobial and deodorization.

This book describes the underlying concepts, potential applications, recent and future development of self-cleaning technologies, and their potential hazards and environmental impacts. It includes:

- Self-cleaning cementitious coatings, glasses, roofing tiles, fibers and fabrics
- Self-cleaning materials for plastic and plastic-containing substrates
- Bactericide textiles
- Nanoscale coatings with self-cleaning properties
- Pulsed laser deposition of surfaces with tunable wettability
- Fabrication of antireflective self-cleaning surfaces

With increasing demand for hygienic, self-disinfecting and contamination-free surfaces, there is much interest in self-cleaning protective materials with applications in medicine, building, environment, optics, aeronautics and space. Self-cleaning road signals, solar panels, car headlights, food packaging, paint, and tents are just some of the possibilities.

 Also available  
as an e-book

**WILEY**

ISBN 978-1-119-99177-9



9 781119 991779